# A Technique for Antenna Configuration Selection for Reconfigurable Circular Patch Arrays

Daniele Piazza, *Student Member, IEEE,* John Kountouriotis, *Student Member, IEEE,* Michele D'Amico, and Kapil R. Dandekar, *Senior Member, IEEE*

***Abstract*—This paper demonstrates a method that allows reconfigurable multi element antennas to select the antenna configuration at the receiver of a Multiple Input Multiple Output (MIMO) communication system. This antenna configuration selection scheme consists of using spatial correlation and average Signal to Noise Ratio (SNR) information to select the antenna radiation pattern at the receiver. We show that using this approach it is possible to achieve capacity gains in a multi element reconfigurable antenna system without modifying the data frame of a conventional MIMO system. We demonstrate our configuration selection algorithm through an analysis of reconfigurable circular patch antennas in realistic MIMO clustered channel models. Using this approach we also show that the functionality of the proposed selection scheme is connected to antenna parameters such as radiation efficiency, input impedance, the level of diversity between the radiation patterns of different antenna configurations, and the average system SNR. The capacity gain achievable with this configuration selection approach is calculated through numerical simulations using reconfigurable circular patch antennas at the receiver of a MIMO system that employs minimum mean square error receivers for channel estimation. The performance of the proposed method is compared to that of a MIMO system that estimates the channel transfer matrix for each antenna configuration in order to select the optimal receiver antenna radiation pattern. Channel capacity and Bit Error Rate (BER) results show the improvement offered by the proposed selection scheme relative to a conventional antenna selection technique for reconfigurable MIMO systems; in particular we show that the improvement increases with the number of configurations in the multi element reconfigurable antenna.**

***Index Terms*—Reconfigurable antennas, multiple input multiple output (MIMO) systems, antenna configuration selection, adaptive communications, smart antennas.**

## I. Introduction

Recent studies have shown that employing reconfigurable antennas can improve the gains offered by Multiple Input Multiple Output (MIMO) systems [1][2][3][4]. These antennas adaptively change their electrical and radiation properties according to the propagation characteristics of the wireless channel in order to provide a "strong" channel between the transmitting and receiving antennas in a given communication system [1][5].

To optimally use such reconfigurable antennas it is necessary to know the channel response between the transmitter and the receiver for each antenna configuration [6]. However, estimating the channel response for each antenna configuration at the transmitter and at the receiver has been demonstrated to be power consuming and to have a detrimental effect on the performance of the reconfigurable MIMO system [6]. The negative effect of channel estimation on the performance of the communication system increases proportionally with the number of antenna configurations, reaching the point where the losses, caused by imperfect channel estimation, may be higher than the capacity gain offered by reconfigurable antennas [6].

In order to overcome this channel estimation problem, we propose a method that allows multi element reconfigurable antennas to select the antenna configuration at the receiver without any extra power consumption and modifications to the data frame of a conventional, non reconfigurable MIMO system. This configuration selection scheme does not aim to maximize the throughput for each particular channel realization, but it selects the antenna configuration that, on average, increases the spectral efficiency of the communication link. While the only existing technique for antenna configuration selection in reconfigurable MIMO antenna systems [6] uses instantaneous channel information to switch antenna configuration, the selection algorithm proposed in this paper is based on second order wireless channel statistics.

The adaptive algorithm we present in this paper is shown to be effective for pattern reconfigurable antennas, though its use can also be extended to other classes of antennas. Pattern reconfigurable antennas are selected because of their advantages in MIMO communications with respect to antennas that exploit space or polarization diversity. Pattern diversity antennas, similarly to polarization diversity antennas, allow system designers to reduce the antenna space occupied on a communication device, solving the size and cost constraints that prevent the antennas from being placed far apart in conventional MIMO systems [5][7]. Also, unlike polarization reconfigurable antennas, pattern reconfigurable antennas can be effectively used without the need for switching antenna configuration at the transmitter and at the receiver simultaneously for polarization alignment. Moreover pattern reconfigurable antennas, unlike polarization reconfigurable antennas,

Manuscript received February 15, 2008; revised June 24, 2008; accepted October 17, 2008. The associate editor coordinating the review of this paper and approving it for publication was J. Tugnait.

D. Piazza, J Kountouriotis, and K. R. Dandekar are with the Department of Electrical and Computer Engineering, Drexel University, Philadelphia, PA 19104-2875 (e-mail: {dp84, jk368, dandekar}@drexel.edu).

M. D'Amico and D. Piazza are with Politecnico di Milano, Dipartimento di Eletronnica e Informazione, Milano 20133 Italy (e-mail: {dpiazza, damico}@elet.polimi.it).

This material is based upon work supported by the U.S. National Science Foundation under grants 0435041 and 0524200.

Digital Object Identifier 10.1109/TWC.2008.080212

allow for the generation of an ideal infinitive number of perfectly uncorrelated patterns per antenna element in order to optimally tune the wireless channel for the highest spectral efficiency.

We present this configuration selection scheme analyzing the performance achievable with reconfigurable circular patch antennas, like the one considered in [5]. As described in [5] these antennas are capable of dynamically changing their patterns by varying the radius of the circular patch. An analysis of the performance of these Reconfigurable Circular Patch Antennas (RCPAs), in terms of ergodic channel capacity and Bit Error Rate (BER), is conducted using the clustered channel model described in [8]. Through this approach we show that the array configuration selection is directly linked to $i)$ the spatial characteristics of the wireless channel (angle spread of the power angular spectrum), $ii)$ the levels of pattern diversity existing between the elements of the reconfigurable array, $iii)$ the differences in radiation efficiency and input impedance between the various antenna configurations, and $iv)$ the average system Signal-To-Noise-Ratio (SNR).

This paper is organized as follows. In Section II we introduce the channel model of a MIMO communication system that employs reconfigurable antennas. In Sections III, we present the reconfigurable antenna used in this paper to study and analyze the performance of the proposed selection scheme. In Section IV we investigate, using the clustered channel model, the dependance of the ergodic channel capacity on the spatial characteristics of the wireless channel, on the differences in radiation efficiency and input impedance between the various antenna configurations of the multi element antenna and on the average system SNR. In Section V we present the novel configuration selection scheme and in Section VI we show the performance achievable with the proposed configuration selection algorithm emphasizing its benefit with respect to existing techniques for multielement reconfigurable antennas. Finally conclusions are drawn in Section VII.

## II. MIMO SYSTEM WITH RECONFIGURABLE ANTENNAS

In this section we describe a MIMO system with M transmit reconfigurable antennas and N receiving reconfigurable antennas, employing spatial multiplexing (SM) transmission scheme. Unlike conventional non reconfigurable multi element antenna systems, in a reconfigurable MIMO system, each antenna element of the transmitting/receving array is capable of changing its radiation pattern characteristics (i.e. pattern, polarization or both). Changing the radiation properties of each antenna element has been shown to be an effective technique to adapt to the changing conditions of the wireless channel in between the transmitter and the receiver [1][2]. By properly selecting the array configuration, it is possible to choose the channel scenario that allows for the highest throughput [1][2].

We consider a MIMO system employing reconfigurable arrays that are capable of $P$ different configurations. Assuming a flat fading channel, the signal collected at the receiver is related to the signal outgoing from the transmitter through the relation:

$$\mathbf{y}_{p,q} = \mathbf{H}_{p,q}\mathbf{x}_{p,q} + \mathbf{n}_{p,q} \tag{1}$$

where $\mathbf{y}_{p,q} \in C^{N\times 1}$ is the signal vector at the receiver array, $\mathbf{x}_{p,q} \in C^{M\times 1}$ is the signal vector at the transmit antenna array, $\mathbf{n}_{p,q} \in C^{N\times 1}$ is the complex additive white Gaussian noise (AWGN) vector with variance $\sigma_n^2$ and $\mathbf{H}_{p,q} \in C^{N\times M}$ is the channel transfer matrix. The subscripts $p$-th and $q$-th refer to the array configuration employed at the transmitter and receiver multi element antenna respectively.

According to the Kronecker model [9], the transfer channel matrix $\mathbf{H}_{p,q}$, is defined as:

$$\mathbf{H}_{p,q} = \mathbf{R}_{RX_q}^{1/2}\mathbf{H}_w\mathbf{R}_{TX_p}^{1/2} \tag{2}$$

where $\mathbf{R}_{TX_p}$ and $\mathbf{R}_{RX_q}$ denote respectively the receive and transmit spatial correlation matrices for the $p$-th configuration of the receiving array and for the $q$-th configuration of the transmitting array respectively. $\mathbf{H}_w \in C^{N\times M}$ is a matrix of complex Gaussian fading coefficients.

To perform estimation of the channel response, $\mathbf{H}_{p,q}$, we consider a pilot assisted estimation that uses minimum mean square error (MMSE) receivers (e.g. [10]). A training sequence composed of $L$ symbols is transmitted with a period of $K$ symbols, and used by the receiver to estimate the channel response. We assume, as is common [11][12][13], that the pilot signals assigned to the different transmit antennas are mutually orthogonal. This assumption implies that the total transmitted data per pilot sequence is equal to $K - LM$ symbols.

We also consider that the transmitted power is uniformly distributed across the $M$ transmit antenna elements. According to [14] we can then express the amplitude of the data symbol as:

$$A = \sqrt{\frac{K}{((K-LM)+\alpha^2 L)}\frac{P_{av}}{M}} \tag{3}$$

where $P_{av}$ is the average transmit power from all transmit antennas and $\alpha$ is a parameter that relates the amplitude of the data symbols to the amplitude of the training symbols $A_p$, so that $A_p = \alpha A$. The percentage of power allocated to the training symbols, $\mu$ is then given by [14]:

$$\mu = \frac{L\alpha^2}{(K-LM)+L\alpha^2}100[\%] \tag{4}$$

For such communication systems, assuming perfect knowledge of the spatial correlation information at the transmitter and at the receiver, we can then define a lower bound of the achievable ergodic channel capacity [15] as:

$$C \geq \frac{K-LM}{K}\times \times E_{\hat{\mathbf{H}}_{p,q}}[\log_2 \det(\mathbf{I} + \frac{P_{av}}{M}\hat{\mathbf{H}}_{p,q}\hat{\mathbf{H}}_{p,q}^{\dagger}(\mathbf{\Upsilon} + \sigma_n^2\mathbf{I})^{-1})] \tag{5}$$

where $\hat{\mathbf{H}}_{p,q}$ is the estimated transfer channel matrix and $\mathbf{\Upsilon}$ is the covariance matrix of the random vector $\mathbf{H_e x_p}$, with $\mathbf{H_e}$ being the MMSE estimation error on $\mathbf{H}_w$ (i.e. $\mathbf{H_e} = \hat{\mathbf{H}}_w - \mathbf{H}_w$); $\mathbf{I}$ is a $N\times N$ identity matrix and $(\dagger)$ denotes a complex conjugate transpose operation. Note that the term $\frac{K-LM}{K}$ is introduced because $L$ temporal signatures per each transmit antenna are allocated to the pilot. The covariance matrix, $\mathbf{\Upsilon}$, is defined as [15]:

$$\mathbf{\Upsilon} = \sigma_{H_e}^2 P_{av}\mathbf{R}_{RX_q} \tag{6}$$

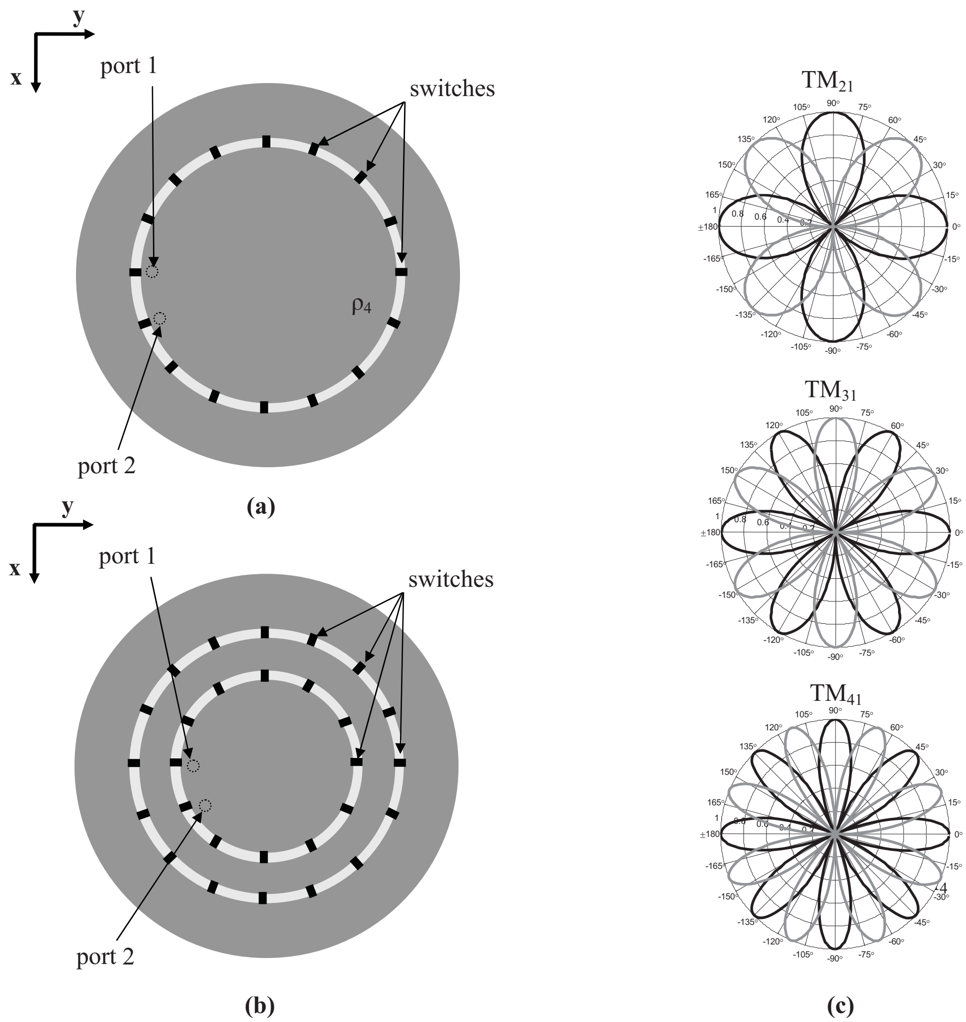


Fig. 1. (a) Schematic of the Reconfigurable Circular Patch Antenna RCPA with two antenna configurations (e.g. $TM_{31}$, $TM_{41}$) and (b) RCPA with three antenna configurations (e.g. $TM_{21}$, $TM_{31}$ and $TM_{41}$). (c) Radiation patterns excited in the azimuthal plane at the two ports of the RCPA for different electromagnetic modes.

where $\sigma^2_{H_e}$ is the variance of the MMSE estimation error on $\mathbf{H}_w$. For this communication system $\sigma^2_{H_e}$ is defined as [10]:

$$\sigma^2_{H_e} = \left( \frac{1}{1 + \frac{\rho_p L_p}{M}} \right) \tag{7}$$

where $\rho_p = \frac{\alpha A}{\sigma_n^2}$ and $L_p$ is the length of the subtraining sequence of $L$, allocated to estimate the channel transfer matrix for a particular antenna configuration at the transmitter and at the receiver [6] ($L_p \in (0, L]$). Note that as $\alpha$ approaches $\infty$ the ergodic channel capacity is that of a system that assumes perfect channel state information at the receiver (p-CSI).

## III. Reconfigurable Circular Patch Antennas

In this section we introduce a multi element reconfigurable antenna that will be used as part of a reconfigurable MIMO system to present a novel antenna configuration selection scheme.

Reconfigurable circular patch antennas (RCPAs) like the one presented in [5] are antennas that can dynamically change the shape of their radiation patterns by varying the size of the circular patch. Each antenna has two feed points and acts as a two element array. As depicted in Fig.1 the two feed points on the antenna structure are separated such that the radiation patterns excited at the two ports are orthogonal to each other. By simultaneously turning on and off the switches located radially on the antenna, it is possible to vary the current distribution on the antenna structure and excite different TM electromagnetic modes, each corresponding to a particular shape of radiation pattern.

As reported in [16], the electric field components excited in the far field by each port of the antenna for the $n$-th TM electromagnetic mode are defined, as a function of the circular patch antenna radius, $\rho$, as:

$$\begin{aligned} E^{(n)}_{\theta,1}(\phi,\theta) =& e^{\frac{jn\pi}{2}} \frac{e^{-jk_0 d}}{d} \frac{V_0}{2} k_0 \rho [J_{n+1}(k_0 \rho \sin\theta) - \\ &- J_{n-1}(k_0 \rho \sin\theta)] \cos[n(\phi - \phi_0)] \end{aligned}$$

$$\begin{aligned} E^{(n)}_{\phi,1}(\phi,\theta) =& - e^{\frac{jn\pi}{2}} \frac{e^{-jk_0 d}}{d} \frac{V_0}{2} k_0 \rho [J_{n+1}(k_0 \rho \sin\theta) + \\ &+ J_{n-1}(k_0 \rho \sin\theta)] \cos\theta \sin[n(\phi - \phi_0)] \end{aligned}$$

$$E^{(n)}_{\theta,2}(\phi,\theta) = e^{\frac{jn\pi}{2}} \frac{e^{-jk_0 d}}{d} \frac{V_0}{2} k_0\rho[J_{n+1}(k_0\rho\sin\theta) - J_{n-1}(k_0\rho\sin\theta)]\sin[n(\phi-\phi_0)]$$

$$E^{(n)}_{\phi_2}(\phi,\theta) = -e^{\frac{jn\pi}{2}} \frac{e^{-jk_0 d}}{d} \frac{V_0}{2} k_0\rho[J_{n+1}(k_0\rho\sin\theta) + J_{n-1}(k_0\rho\sin\theta)]\cos\theta\cos[n(\phi-\phi_0)]$$

where $E_{\theta,<1,2>}$ and $E_{\phi,<1,2>}$ are the $\theta$ and $\phi$ components of the electric fields excited at port 1 and port 2 of the RCPA. $J_n(k_0\rho\sin\theta)$ is the Bessel function of the first kind and order $n$, $\phi_0$ is the reference angle corresponding to the feed point location on the antenna, $V_0$ is the edge voltage at $\phi = 0$, $k_0$ is the wavenumber, and $d$ is the distance from the antenna. Varying the radius of the antenna, different electromagnetic modes can be excited according to [16]:

$$\rho = \frac{\chi_n^{'}\lambda}{2\pi\sqrt{\varepsilon_r}} \tag{8}$$

where $\varepsilon_r$ is the dielectric permittivity of the substrate, $\lambda$ is the wavelength and $\chi_n^{'}$ is the first zero of the derivative of the Bessel function $J_n$.

In this paper we will consider RCPAs capable of exciting three different electromagnetic modes (i.e. configurations) at both ports: $TM_{21}$, $TM_{31}$ and $TM_{41}$. The radiation patterns that are excited in the azimuthal plane with such RCPAs are shown in Fig.1(c). We note that the patterns excited at the two ports of the RCPA, for the same antenna configuration, are orthogonal to each other and that variations between radiation patterns of different RCPA modes occur in the number of lobes and in their beamwidth. To quantify the level of diversity existing between radiation patterns excited at the ports of the RCPA, we use the spatial correlation coefficient, $\hat{r}_{j,k,l,m}$, defined as [17]

$$\hat{r}_{j,k,l,m} = \frac{\int_{4\pi} P(\Omega)\underline{E}_{j,k}(\Omega)\underline{E}^{\dagger}_{l,m}(\Omega)d\Omega}{\left[\int_{4\pi} P(\Omega)|\underline{E}_{j,k}(\Omega)|^2 d\Omega \int_{4\pi} P(\Omega)|\underline{E}_{l,m}(\Omega)|^2 d\Omega\right]^{1/2}} \tag{9}$$

where $j$ and $l$ define the array port and $k$ and $m$ the antenna configuration at the port $j$ and $l$ respectively. $\underline{E}_{j,k}(\Omega)$ is the radiation pattern of the configuration $k$ at port $j$ over the solid angle $\Omega = (\phi,\theta)$. $P(\Omega)$ is a probability density function that describes the incident multipath field distribution. For a rich scattering environment, $P(\Omega)$ is uniformly distributed over $\Omega$ (i.e. $P(\Omega) = \frac{1}{4\pi}$) [17]. Table I shows the level of diversity existing between radiation patterns excited at the two ports of the array for each antenna configuration ($\hat{r}_{1,k,2,k}$), while Table II reports the level of diversity existing between the different antenna configurations ($\hat{r}_{1,k,1,m}$). We observe that the correlation values between radiation patterns excited at the two ports of the array are small enough for all the configurations ($\leq 0.7$) to provide significant diversity gain [18]. Table II shows that the correlation between different configurations is about 0.8 for all the states. Although this value is large, as shown in [5] and in Section VI, the differences between the array configurations are high enough to provide an improvement in terms of spectral efficiency and BER with respect to non reconfigurable circular patch antennas.

TABLE I
SPATIAL CORRELATION BETWEEN PATTERNS GENERATED AT TWO DIFFERENT PORTS OF THE RCPA FOR THE SAME CONFIGURATION - $\hat{r}_{1,k,2,k}$

| $\hat{r}_{1,TM_{21},2,TM_{21}}$ | $\hat{r}_{1,TM_{31},2,TM_{31}}$ | $\hat{r}_{1,TM_{41},2,TM_{41}}$ |
|---|---|---|
| 0.63 | 0.63 | 0.63 |

TABLE II
SPATIAL CORRELATION BETWEEN PATTERNS GENERATED AT THE SAME PORT OF THE RCPA - $\hat{r}_{1,k,1,m}$

| | $\underline{E}_{1,TM_{21}}$ | $\underline{E}_{1,TM_{31}}$ | $\underline{E}_{1,TM_{41}}$ |
|---|---|---|---|
| $\underline{E}_{1,TM_{21}}$ | 1 | 0.80 | 0.85 |
| $\underline{E}_{1,TM_{31}}$ | 0.80 | 1 | 0.81 |
| $\underline{E}_{1,TM_{41}}$ | 0.85 | 0.81 | 1 |

Differences between the various antenna configurations (and electromagnetic modes) exists not only in the shape of the excited radiation patterns, but also in the level of radiation efficiency, $\eta$, defined as:

$$\eta = \frac{Q_T}{Q_R} \tag{10}$$

where $Q_T$ is the antenna total quality factor and $Q_R$ is the radiation quality factor; $Q_T$ takes into account dielectric, conduction and radiation losses while $Q_R$ is a figure of merit for only the radiation losses. They are defined, for a circular patch antenna, as [19]:

$$Q_T = \left(\frac{1}{h\sqrt{\pi\mu f\sigma}} + \tan\delta + \frac{h\mu f(k_0\rho)^2 I_1}{240[\chi_n^{'2} - n^2]}\right)^{-1} \tag{11}$$

$$Q_R = \left(\frac{240[\chi_n^{'2} - n^2]}{h\mu f(k_0\rho)^2 I_1}\right) \tag{12}$$

where $f$ is the frequency of operation, $\mu$ is the substrate dielectric permeability, $h$ is the substrate thickness and $\sigma$ is the conductivity of the material used to build the circular patch. $\tan\delta$ is a figure of merit that takes into account the substrate losses and $I_1$ is defined as:

$$I_1 = \int_0^{\pi} \Big[\big(J_{n+1}(k_0\rho\sin\theta) - J_{n-1}(k_0\rho\sin\theta)\big)^2 + (\cos\theta)^2\big(J_{n+1}(k_0\rho\sin\theta) + J_{n-1}(k_0\rho\sin\theta)\big)^2\Big]\sin\theta d\theta \tag{13}$$

In Fig.2 the radiation efficiency is reported as a function of the dielectric permittivity for different configurations of a RCPA matched at 5.2 $GHz$ and built on a substrate of thickness $h = 0.159\ mm$ and $\tan\delta = 0.0009$. It can be observed that the level of radiation efficiency is different for each antenna configuration, as is true for most of the electrically reconfigurable antennas proposed in the literature. For the RCPAs we can note that the lower electromagnetic modes are more efficient than the higher modes. Also we observe that when the dielectric permittivity value increases, the radiation efficiency decreases. In this paper we will consider two different types of RCPAs that differ in antenna substrate and level of radiation efficiency. A summary of the main characteristics of these two antennas is reported in Table III.

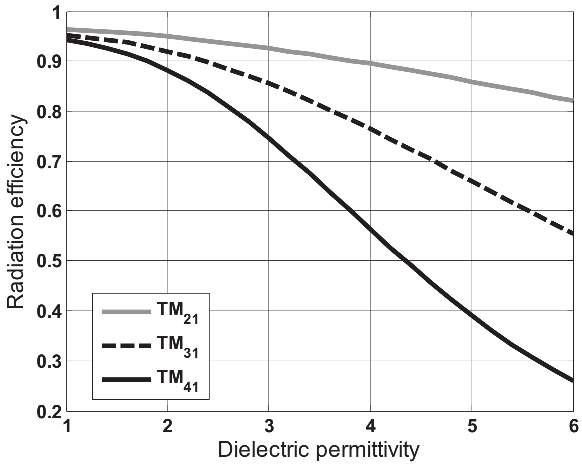


Fig. 2. RCPA radiation efficiency for different antenna configurations as a function of the substrate dielectric permittivity. $h = 1.59$ mm, $\sigma = 5.8 \times 10^7$ S/m, $f = 5.2$ GHz and $tan\delta = 0.0009$.

TABLE III
RCPAs CHARACTERISTICS

| | RCPA-1 | RCPA-2 |
|---|---|---|
| substrate | Rogers RT-duroid 5880 | Rogers R03003 |
| $\varepsilon_r$ | 2.2 | 3 |
| $\eta_{TM_{21}}$ | 0.94 | 0.88 |
| $\eta_{TM_{31}}$ | 0.91 | 0.81 |
| $\eta_{TM_{41}}$ | 0.87 | 0.66 |
| $\rho_{TM_{21}}$ | $0.33\lambda$ | $0.28\lambda$ |
| $\rho_{TM_{31}}$ | $0.45\lambda$ | $0.39\lambda$ |
| $\rho_{TM_{41}}$ | $0.57\lambda$ | $0.49\lambda$ |
| $S_{11}$ | 0 | 0 |

## IV. RCPAs PERFORMANCE IN CLUSTERED CHANNEL MODEL

In this section we show how the ergodic channel capacity is related to angle spread of the wireless channel power angular spectrum, antenna radiation efficiency, level of pattern diversity, input impedance of each antenna configuration and average system SNR. We first describe the adopted clustered channel model and then we separately analyze the effect of spatial correlation and average system SNR on the channel spectral efficiency.

### A. Clustered channel model and RCPA spatial correlation

We describe the wireless channel according to the cluster channel model presented in [8]. Each cluster is characterized by a mean angle of arrival (AOA) $\Omega_c$, where $\Omega_c = (\phi_c, \theta_c)$ represents the solid angle consisting of azimuth ($\phi_c$) and elevation ($\theta_c$) components. Depending on the system bandwidth, the excess delay across different propagation paths may not be resolvable. In this case, multiple AOAs are defined with an offset $\phi$ with respect to the mean AOA of the cluster ($\phi_c$). This angle of arrival is generated according to a certain probability density function (PDF) that models the power angular spectrum (PAS). The variance of the PAS is a measure of the angle spread (AS), $\sigma_\phi$, of the cluster.

We define the PAS as $P(\Omega) = P_\phi(\Omega) + P_\theta(\Omega)$, where $P_\phi$ and $P_\theta$ are the angular power densities of the $\hat{\phi}$ and $\hat{\theta}$ components of the incident field, respectively. It is also assumed, consistent with the measurement results in [20], that most of the scattered power propagates over the azimuth directions. Therefore $P(\Omega) = Q(\Omega) * \delta(\phi - \phi_c)\delta(\theta - \pi/2)$, where $*$ denotes the convolution operator and $Q(\Omega)$ is generated according to the truncated Laplacian distribution as in [8].

As described in [1] we can define, from (9), the spatial correlation between the $k$-th and $m$-th pattern configuration excited at the $j$-th and $l$-th ports of multi element antennas, including the effect of the wireless channel, as:

$$\begin{aligned} r_{j,k,l,m} &= \\ &= \sqrt{(1-|S_{11_j}|^2)\eta_{j,k}(1-|S_{11_l}|^2)\eta_{l,m}} \times \hat{r}_{j,k,l,m} = \\ &= \sqrt{(1-|S_{11_j}|^2)\eta_{j,k}(1-|S_{11_l}|^2)\eta_{l,m}} \times \\ &\times \frac{\int_{4\pi} P(\Omega)\underline{E}_{j,k}(\Omega)\underline{E}^{\dagger}_{l,m}(\Omega)d\Omega}{\int_{4\pi} P(\Omega)|\underline{E}_{ref}(\Omega)|^2 d\Omega} \end{aligned} \tag{14}$$

where we have set

$$\left[\int_{4\pi} P(\Omega)|\underline{E}_{j,k}(\Omega)|^2 d\Omega \int_{4\pi} P(\Omega)|\underline{E}_{l,m}(\Omega)|^2 d\Omega\right]^{1/2} = \\ = \int_{4\pi} P(\Omega)|\underline{E}_{ref}(\Omega)|^2 d\Omega,$$

with $\underline{E}_{ref}(\Omega)$ being the electric field of a reference antenna configuration that is used as normalization factor for the spatial correlation coefficient. $S_{11}$ is the voltage reflection coefficients at the antenna input ports and $\eta$ is the antenna radiation efficiency.

According to [7] we can then write the theoretical spatial correlation coefficients of a two port RCPA as:

$$\begin{aligned} r_{l,m,l,m}(\phi_c,\sigma_\phi) = &\frac{(1-|S_{11_{l,m}}|)\eta_{l,m}}{(1-e^{-\sqrt{2}\pi/\sigma_\phi})} \frac{(n\sigma_\phi)^2}{1+2(n\sigma_\phi)^2} \times \\ &\times \left[1 - e^{-\sqrt{2}\pi/\sigma_\phi} + \frac{\cos^2(n\phi_c)}{(n\sigma_\phi)^2} \times \right. \\ &\left. \times \left(1 - e^{-\sqrt{2}\pi/\sigma_\phi}\cos(n\pi)\right)\right] \end{aligned} \tag{15}$$

$$\begin{aligned} r_{j,k,j,k}(\phi_c,\sigma_\phi) = &\frac{(1-|S_{11_{j,k}}|)\eta_{j,k}}{(1-e^{-\sqrt{2}\pi/\sigma_\phi})} \frac{(n\sigma_\phi)^2}{1+2(n\sigma_\phi)^2} \times \\ &\times \left[1 - e^{-\sqrt{2}\pi/\sigma_\phi} + \frac{\sin^2(n\phi_c)}{(n\sigma_\phi)^2} \times \right. \\ &\left. \times \left(1 - e^{-\sqrt{2}\pi/\sigma_\phi}\cos(n\pi)\right)\right] \end{aligned} \tag{16}$$

$$\begin{aligned} r_{j,k,l,m}(\phi_c,\sigma_\phi) = &\frac{\sqrt{(1-|S_{11_{l,m}}|)\eta_{l,m}(1-|S_{11_{j,k}}|)\eta_{j,k}}}{2} \\ &\times \frac{(\sin n\phi_c)}{1+2(n\sigma_\phi)^2} \end{aligned} \tag{17}$$

where we have assumed $\int_{4\pi} P(\Omega)|\underline{E}_{ref}(\Omega)|^2 d\Omega = 1$. We observe that the input impedance, efficiency and AS of the power angular spectrum describing the wireless channel, act as scaling factors of the spatial correlation coefficient.

Knowing the spatial correlation coefficient for each antenna configuration allows us to compute the transfer channel matrix $\mathbf{H}_{p,q}$ as in (2). In this paper, we will consider only single sided correlated MIMO channels. In particular, we use RCPAs only at the receiver while at the transmitter we assume

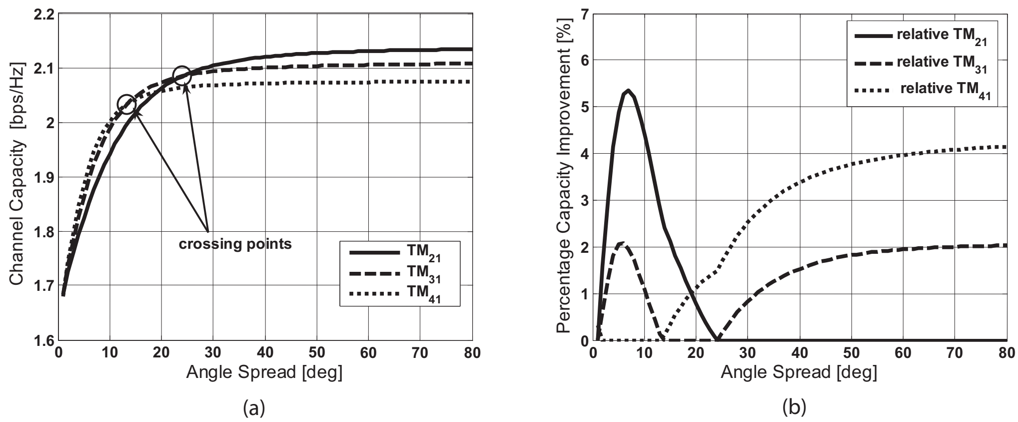


Fig. 3. (a) Channel capacity curves for three different antenna configurations ($TM_{21}$, $TM_{31}$ and $TM_{41}$) as a function of the angle spread (AS) for a $2 \times 2$ MIMO system employing the RCPA-1 at the receiver. (b) Percentage capacity improvement, as a function of the angle spread (AS), achievable when using the RCPA-1 in the same $2 \times 2$ MIMO system relative to a non reconfigurable antenna system employing circular patch antennas operating in mode $TM_{21}$, $TM_{31}$ and $TM_{41}$. SNR = 5 dB.

$\mathbf{R}_{TX} = \mathbf{I}$. We make this assumption because we present an antenna configuration selection technique for the receiver, independently from the transmitter. The fact that $\mathbf{R}_{TX} = \mathbf{I}$ does not affect the following analysis, which would not change for $\mathbf{R}_{TX} \neq \mathbf{I}$.

The ergodic channel capacity achievable for each RCPA configuration can then be calculated according to equation (5) for the case of perfect channel state information at the receiver ($\alpha \longrightarrow \infty$), as discussed in Section II. The following analysis is performed in the single cluster channel model and the spatial correlation information is determined as in (14), using configuration $TM_{21}$ as a reference antenna.

### *B. Effect of RCPA spatial correlation on configuration selection*

In Fig.3(a) the average channel capacity achievable for some configurations of a reconfigurable circular patch antenna is reported as a function of the AS of the PAS, for a SNR = 5 $dB$. The ergodic channel capacity values are averaged over all azimuthal angles ($\phi_c \in [0, 2\pi)$) of the incoming PAS. Note that these results of channel capacity have been determined for a RCPA built on a Rogers RT-duroid 5880 substrate and for a condition of perfect matching for all the antenna configurations (RCPA-1). Refer to Table III for a summary of the antenna related parameters. We observe that the achievable average channel capacity varies as a function of the PAS angle spread. In particular each antenna configuration outperforms the others for a certain range of angle spread. In Fig.4 we show the same ergodic channel capacity of Fig.3(a) for a RCPA built on Rogers R03003 substrate (RCPA-2). The parameters for RCPA-2 are also described in Table III. As shown in this table, RCPA-2 is characterized by different values of radiation efficiency with respect to RCPA-1. A comparison of Fig.3(a) with Fig.4 shows that the crossing points of the channel capacity traces vary as a function of the radiation efficiency of the configuration. This effect can be better explained by looking at the average channel capacity curves relative to an ideal RCPA having unit efficiency for all its configurations (Fig.4 (b)). We note that, in this case, configuration $TM_{41}$ outperforms the other configurations for low AS while for large AS all the configurations perform the same. This happens because, at low AS, higher order modes are characterized by larger pattern diversity with respect to lower modes, while at high AS, the level of pattern diversity is similar for all the antenna modes, as demonstrated in [7]. On the other hand, the radiation efficiency, that is larger for lower order modes than for higher modes, determines configuration $TM_{21}$ to have the best performance at high AS, as depicted in Fig.3(a) and Fig.4. A similar conclusion could be drawn if we considered a variation in input impedance among the different antenna configurations. In fact, according to equations (15), (16) and (17), the antenna matching condition (represented by $S_{11}$) scales the spatial correlation coefficients in the same way as the efficiency.

These results demonstrate the possibility of selecting the antenna configuration at the receiver based on PAS angle spread knowledge, once the average system SNR is known. In Fig.3(b) we show the percentage capacity improvement achievable when using RCPAs relative to a non reconfigurable antenna system (i.e. fixed radius circular patch antennas operating in mode $TM_{21}$, $TM_{31}$ and $TM_{41}$). It can be noted that, for the system of Fig.3(b), using angle spread information to switch between configurations leads to an average improvement of up to 5% with respect to a system that does not employ reconfigurable antennas.

### *C. Effect of average system SNR on configuration selection*

As shown in (5) the ergodic channel capacity of a MIMO system does not depend only on the spatial correlation, but also on the system average SNR. In Fig.5 the average channel capacity achievable for the different configurations of RCPA-1 is shown as a function of the AS of the PAS, for a SNR = 20 $dB$ (Fig.5(a)) and SNR = 0 $dB$ (Fig.5(b)). We note that the achievable channel capacity is, as expected, higher for the system with SNR = 20 $dB$ than that of the same system with average SNR = 5 $dB$ (Fig.8(a)) and SNR = 0 $dB$. We also observe that the angle spread crossing points of the capacity curves, for different antenna configurations, shift with varying

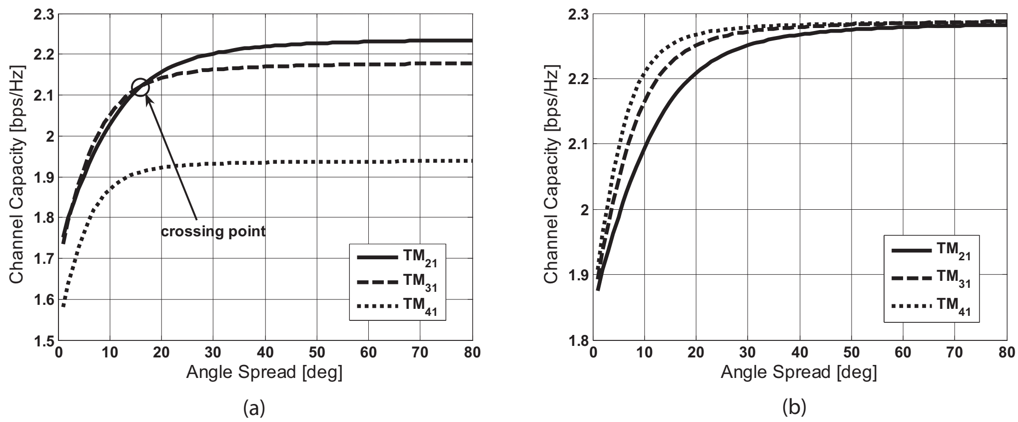


Fig. 4. Channel capacity curves for three different antenna configurations ($TM_{21}$, $TM_{31}$ and $TM_{41}$) as a function of the angle spread (AS) for a $2 \times 2$ MIMO system employing (a) the RCPA-2 at the receiver, (b) an ideal RCPA with unitary radiation efficiency for all the antenna configurations. SNR = 5 dB.

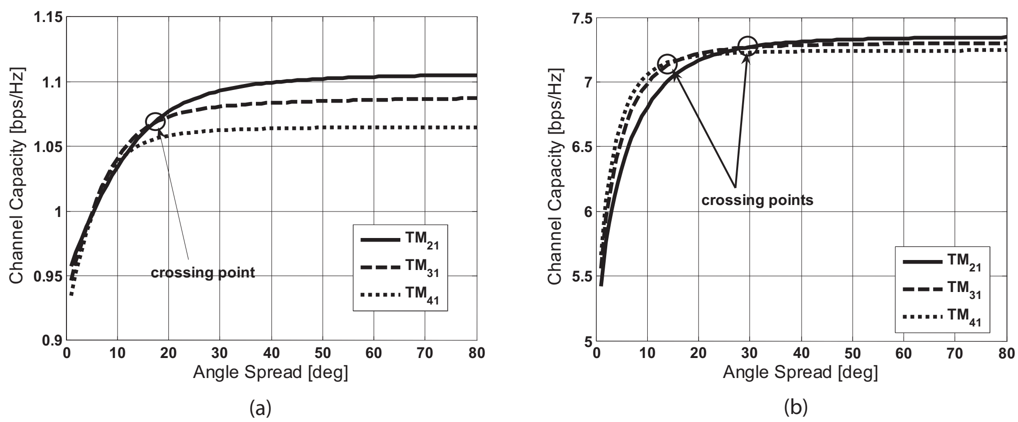


Fig. 5. Channel capacity curves for three different antenna configurations ($TM_{21}$, $TM_{31}$ and $TM_{41}$) as a function of the angle spread (AS) for a $2 \times 2$ MIMO system employing the RCPA-1 at the receiver. (a) SNR = 0 dB, (b) SNR = 20 dB.

average system SNR. Using the same reconfigurable antenna, at SNR = 20 $dB$, the AS crossing points values are higher with respect to a system with SNR = 0 $dB$.

In Fig.6 the AS crossing points for configurations $TM_{41} - TM_{31}$ and $TM_{31} - TM_{21}$ are reported as a function of the system average SNR, for a MIMO system that employs RCPA-1 at the receiver. We observe that as the value of average system SNR increases, the AS crossing point values increase as well. This effect can be explained if we consider that the channel capacity of MIMO systems can be increased in two ways: $i)$ increasing the system diversity and $ii)$ increasing the amount of signal power received. The system diversity is reflected in the antenna correlation coefficient, while the signal power received is influenced by the antenna efficiency and input impedance. Intuitively, at high SNR, since the received amount of power can not be greatly modified by varying the antenna efficiency and input impedance, the level of antenna diversity is the dominant contribution to the achievable channel capacity. At low SNR, instead, small variation in antenna efficiency and input impedance can greatly effect the amount of received signal power, and therefore antenna efficiency and input impedance are dominant contributions on the channel capacity trend. As shown in Fig.5(a) we note that at low SNR the most efficient antenna ($TM_{21}$) has larger advantage with respect to the other configurations. On the other hand at high SNR (Fig.5(b)) the configuration with the lowest spatial correlation ($TM_{41}$) outperforms the others for more values of angle spread with respect to the same system at lower SNR.

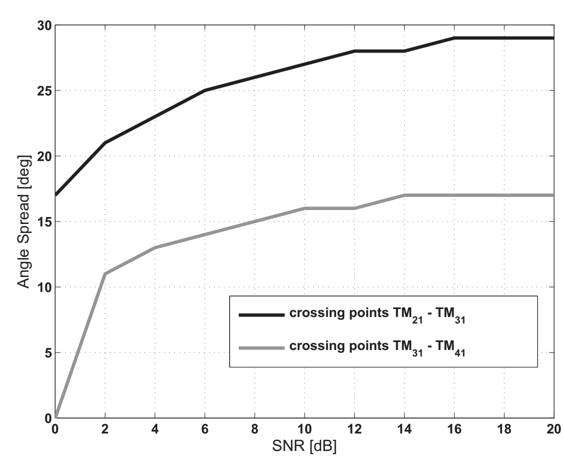


Fig. 6. Angle spread crossing points versus SNR for configurations $TM_{21} - TM_{31}$ and $TM_{31} - TM_{41}$.

These results demonstrate therefore the possibility of selecting the antenna configuration at the receiver based on knowledge of PAS angle spread and average system SNR.

## V. Selection Algorithm

In this section we introduce a selection algorithm for multi element reconfigurable antenna arrays that would allow the system to select receiver antenna configuration using second order channel statistics and average SNR information.

A parameter of discrimination between the different wireless channel scenarios is the reciprocal condition number of the transmit/receive correlation matrices, defined as [21][22]:

$$D_\lambda = \frac{\lambda_{max}}{\lambda_{min}} \tag{18}$$

where $\lambda_{max}$ and $\lambda_{min}$ are the maximum and minimum eigenvalues of the transmit and receive correlation matrices.

In Fig.7 reciprocal condition number is plotted as a function of the angle spread of the PAS for a RCPA (RCPA-1) operating in mode $TM_{21}$. For each value of AS, there is a corresponding value of reciprocal condition number; in particular for low values of AS the reciprocal condition number is high and vice-versa. We can therefore map, given the average system SNR, the values of AS that define a switching point between two configurations (as shown in Fig.3(a)) to reciprocal condition number. In Table IV, a mapping of reciprocal condition number to corresponding values of AS regions is presented. Note that, given the results of Fig.3(a), only three regions of $D_\lambda$ need to be specified; each region corresponds to a particular antenna configuration at the receiver. This mapping procedure is necessary since the PAS angle spread is difficult to estimate, while the transmit/receive spatial correlation matrices can be estimated using standard techniques [23][24]. Note that the mapping procedure varies with the average system SNR, as explained in Section IV-C. Therefore an antenna table, like the one of Table IV, need to be generated for each average SNR value.

According to this channel parametrization, it is therefore possible to use second order wireless channel statistics together with the average SNR, in order to determine receiver array configuration. Note that this approach allows the system to select the antenna configuration using the spatial correlation matrix of only one reference antenna configuration without the need of estimating the channel response over each antenna configuration. This greatly simplifies channel estimation in reconfigurable MIMO systems (discussed further in Section VI). In the example of Table IV the antenna configuration $TM_{21}$ has been selected as arbitrary reference antenna.

An algorithm that allows for the selection of the antenna configuration at the receiver, without estimating the channel transfer matrix for each antenna configuration, can then be summarized as follows:

OFF LINE OPERATIONS

**1**. Antenna tables, like the one of Table IV, that maps the optimal antenna configuration at the receiver to the range of reciprocal number are built, one for each average SNR value, using the clustered channel model approach described in Section IV.

ON LINE OPERATIONS

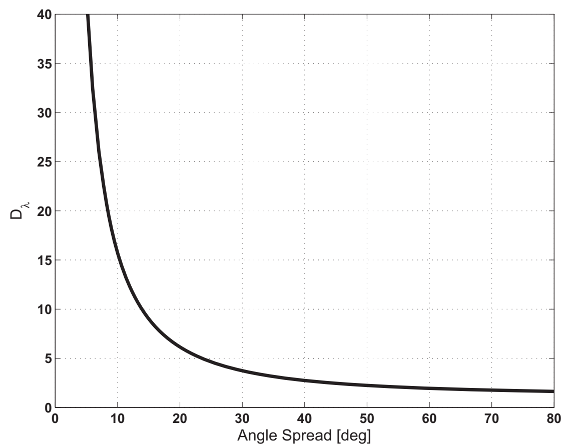


Fig. 7. Reciprocal condition number, $D_\lambda$, as a function of the angle spread for the antenna configuration $TM_{21}$ used at the receiver in a $2 \times 2$ MIMO system.

TABLE IV
Relationship of Angle Spread to Reciprocal Condition Number for SNR = $5dB$

| AS | $D_\lambda$ | CONFIGURATION |
|---|---|---|
| $[0^o, 13^o)$ | $(11, \infty)$ | $TM_{41}$ |
| $[13^o, 23^o)$ | $(5, 11]$ | $TM_{31}$ |
| $[23^o, 360^o)$ | $(0, 5]$ | $TM_{21}$ |

**2**. The average system SNR is determined and used to select the corresponding antenna table generated in step 1.

**3**. The receiver spatial correlation is determined for the reference receiver antenna configuration which is used to determine the channel reciprocal condition number, $D_\lambda$.

**4**. The information of the reciprocal condition number, $D_\lambda$, is used together with the antenna table generated in step 1 to select the antenna configuration at the receiver.

We observe that the proposed selection algorithm requires the channel second order statistics to be constant over the configuration selection procedure [25]. Estimation of the spatial correlation matrix could then be conducted using standard techniques [23][24]. Once the channel correlation is estimated and the antenna configuration is selected, the $L$ symbols of the pilot sequence can be used to estimate the channel for signal detection as discussed in Section II.

## VI. Effect of Pilot Assisted Estimation on the Channel Capacity and BER

In this section the performance achievable with the proposed configuration selection scheme is evaluated for a MIMO system like the one described in Section II, including the effect of imperfect channel estimation (np-CSI) ($\alpha$ finite), in terms of ergodic channel capacity and BER. We also compare the performance of such a selection scheme to that achievable with a system that detects the optimal antenna configuration by exhaustively estimating the channel transfer matrix for every possible antenna configuration [6]. According to the system in [6], the results presented in this section are based on the frame structure of the IS-136 standard. IS-136 is based on Time Division Multiple Access (TDMA) technology where

TABLE V
MIMO SYSTEM CONFIGURATION

| | $2 \times 2$ MIMO | $2 \times 6$ MIMO |
|---|---|---|
| RCPA type | RCPA-1 | RCPA-1 |
| array configurations states (P) | 3 | 10 |
| $\mu_{proposed\ algorithm}$ | 6% | 11% |
| $\alpha_{proposed\ algorithm}$ | 0.44 | 0.58 |
| $\mu_{standard\ algorithm}$ | 10% | 20% |
| $\alpha_{standard\ algorithm}$ | 0.61 | 0.88 |

each frame length is 40 ms. Each IS-136 frame consists of $K$ = 162 symbols, of which $L$ = 32 symbols are used for training purposes.

In case of a configuration selection scheme like the one described in [6], in order to evaluate the optimal antenna configuration, the $L$ symbols allocated for channel estimation are subdivided into $P$ subtraining sequences of length $L_p = \frac{L}{P}$, where $P$ is the number of array configurations at the receiver. Each subtraining sequence is used to estimate the transfer channel matrix for a particular antenna configuration. According to this approach the achievable ergodic capacity can then be computed as described in equation (5).

Note that contrary to this selection approach, the selection algorithm proposed in this paper always has $L_p = L$ independently of the number of receiver antenna configurations. In this way, a better estimation of the channel matrix can be obtained, resulting in better signal detection, and therefore, higher achievable channel capacity and lower BER. The technique in [6] always selects the optimal antenna configuration based on the channel scenario that maximizes the receive signal-to-noise ratio, while the proposed selection scheme selects the antenna configuration that on average increases the spectral efficiency of the communication link.

### A. Ergodic channel capacity

In Fig.8(a) the channel capacity achievable with a RCPA (RCPA-1) employed at the receiver of a $2 \times 2$ MIMO link is reported as a function of the AS, for a system that employs the proposed selection scheme including the effects of imperfect channel estimation (proposed algorithm np-CSI) or assuming perfect channel estimation (proposed algorithm p-CSI) ($\alpha \to \infty$). The Figure also shows results for a system that selects the antenna configuration after exhaustively estimating the channel for each configuration including the effects of imperfect channel estimation (standard np-CSI) or assuming perfect channel estimation (standard p-CSI). These results are obtained for $P_{av} = 1$, a SNR = 5 dB, and an allocated power to the training sequence, $\mu$, optimal for each selection scheme. A summary of the system configuration is shown in Table V. Note that the adopted RCPA is capable of switching between modes $TM_{21}$, $TM_{31}$ and $TM_{41}$ and thus in this case $P$ = 3. It can be observed that the imperfect channel estimation causes a decrease in overall system performance. Note in particular, that the loss in capacity is higher for the selection scheme that needs to estimate the channel $P$ times (one estimation per antenna configuration) every training sequence than for the proposed approach that instead estimates the channel only for a single antenna configuration. The percentage capacity improvement achievable when using such a selection scheme with RCPAs is reported in Fig.8(b) relative to non reconfigurable antenna systems operating in different modes, and an RCPA system that selects the antenna configuration after exhaustively estimating the channel for all possible configurations. In terms of its ergodic capacity, on average the improvement achievable with the proposed selection algorithm is 9% with respect to technique in [6]. Note also that using the RCPAs at the receiver together with the technique in [6] performs worse than employing non reconfigurable circular patch antennas. This happens because, using the technique in [6], the imperfection in channel estimation is so high so as to appreciably decrease the system achievable channel capacity. Note in fact that, according to the technique in [6], as the number of receiver antenna configurations increases, the imperfection in channel estimation increases and consequently the achievable channel capacity decreases.

In Fig.9 the channel capacity achievable with the proposed selection scheme is determined for a $2 \times 6$ MIMO system employing RCPAs only at the receiver for a SNR = 5dB. The MIMO system configuration is shown in Table V. In this case three RCPAs, built on Rogers RT-duroid 5880 substrate (RCPA-1), are used at the receiver with spatial separation of multiple wavelengths, such as to be uncorrelated one with the other. A total of ten possible array configurations can then be selected at the receiver ($P = 10$[1]), using a RCPA that is capable of switching between modes $TM_{21}$, $TM_{31}$ and $TM_{41}$. At the transmitter we assume $\mathbf{R}_{TX} = \mathbf{I}$. Since the number of antenna configurations is higher than the $2 \times 2$ MIMO case (where $P$ = 3) the capacity improvement achievable using the proposed selection scheme is higher. The improvement is in fact almost $20\%$. As explained in [6], the greater the number of array configurations, the worse the channel transfer matrix detection, and therefore the worse the channel capacity. This problem is addressed by the proposed selection scheme that needs to estimate the channel for a single antenna configuration independently of the number of array configurations.

### B. Bit Error Rate

An analysis of the proposed configuration selection algorithm performance, in terms of BER, has been conducted for a $2 \times 2$ MIMO system employing RCPA-1 antennas at the receiver. The modulation scheme considered is BPSK without any additional coding. BER values have been calculated assuming perfect decoupling at the receiver of the two Single Input Single Output (SISO) links comprising the $2 \times 2$ MIMO system.

In Fig10(a) BER curves are reported as a function of the SNR for an angle spread of $10^o$. The reported curves are specific to: $i$) a system that employs the proposed selection scheme including the effects of imperfect channel estimation (proposed algorithm np-CSI), $ii$) a system that selects the antenna configuration after exhaustively estimating the channel for each configuration including the effects of

[1]P is determined as the combinations of the number of configurations, $K$, per RCPA that can be repeated up to $J$ times in the array. $P = \frac{(K+J-1)!}{J!(K-1)!}$. In case of six elements antenna array at the receiver, three RCPA are used and therefore $J = 3$. In this case, using an RCPA with three different configurations ($K$ = 3), we obtained $P = 10$.

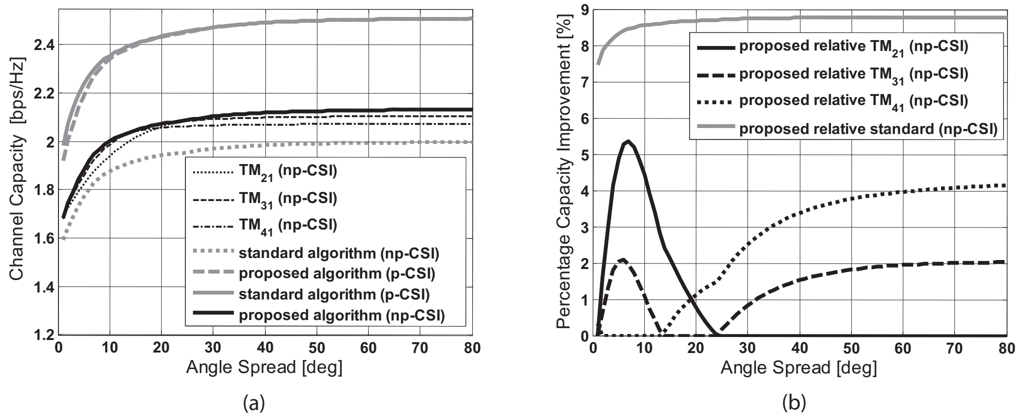


Fig. 8. (a) Achievable channel capacity as a function of the angle spread (AS) for a $2 \times 2$ MIMO system, with RCPA-1 at the receiver, that employs:(i) the proposed selection scheme including the effects of imperfect channel estimation (proposed algorithm np-CSI), (ii) the proposed selection scheme assuming perfect channel estimation (proposed algorithm p-CSI), (iii) an algorithm that selects the antenna configuration after estimating the channel for all possible configuration including the effects of imperfect channel estimation (standard np-CSI) and, (iv) a standard algorithm assuming perfect channel estimation (standard p-CSI). The curves relative to the channel capacity achievable with non reconfigurable circular patch antennas operating in different modes assuming non-perfect channel estimation are also reported. (b) Percentage capacity improvement, as a function of the angle spread (AS), for the same $2 \times 2$ MIMO system that employs RCPA-1 at the receiver with the proposed selection algorithm relative to non reconfigurable antenna systems operating in different modes (proposed relative $TM_{21}$, $TM_{31}$ and $TM_{41}$) and RCPA system that selects the antenna configuration after exhaustively estimating the channel for all possible configurations (proposed relative standard (np-CSI)). SNR = 5 dB.

imperfect channel estimation (standard algorithm np-CSI) and, $iii)$ a system assuming perfect channel estimation (standard algorithm p-CSI). The Figure also shows results for a system equipped with non reconfigurable circular patch antennas operating in modes $TM_{21}$, $TM_{31}$ and $TM_{41}$. We note that the proposed algorithm achieves an appreciable gain with respect to a standard selection algorithm that selects the antenna configuration after exhaustively estimating the channel for each configuration. In particular we note that a gain of 1.8 dB is achieved for a BER of 0.1. This gain is not due to an improvement in the diversity order of the system, but to the fact that with the proposed algorithm the channel is better estimated than with the standard algorithm. Specifically, in the proposed algorithm, the training sequence is entirely allocated to estimate the channel for a single antenna configuration, instead of being allocated to estimate the channel for all possible array configurations. This effect can be better observed by comparing the BER curve of a system with perfect channel estimation (standard algorithm p-CSI) with the BER curves of systems with imperfect channel estimation (proposed algorithm np-CSI and standard algorithm np-CSI). In Fig10(a) we observe that in systems with imperfect channel estimation the BER curves are shifted to the right at higher SNR. To explain this result we note that imperfect channel estimation impacts the SNR level at the receiver [6]. In particular, for a system that selects the antenna configuration after exhaustively estimating the channel for each configuration, the quality of channel estimation diminishes as the number of array configurations, P, is increased. Thus the SNR level at the receiver is degraded [6]. Unlike a standard algorithm, the proposed configuration selection scheme, estimates the channel for a single antenna configuration and therefore the quality of channel estimation remains the same, independent of the number of array configurations. This improved channel estimaion leads to a better SNR level at the receiver. Note also that the BER curve slope for the proposed algorithm is less steep than the one corresponding to the standard algorithm; therefore the diversity order of the system that uses the proposed algorithm is degraded with respect to a system that uses the standard algorithm. This diversity order degradation is due to the fact that the proposed selection algorithm does not select the optimal antenna configuration for each particular channel realization, but it selects the antenna configuration that, on average, increases the spectral efficiency of the communication link. Finally we observe that in the case of low angle spread (e.g. AS=$10^o$), the proposed algorithm always selects configuration $TM_{41}$, which is the one that on average outperforms the other configurations in terms of channel capacity.

In Fig.10(b) the same BER curves are shown for an angle spread of $60^o$. A similar gain is achieved using the proposed algorithm with respect to a system that selects the antenna configuration after exhaustively estimating the channel for each configuration. However we observe that, different from the case of Fig.10(a), at high AS the proposed algorithm always selects configuration $TM_{21}$. Recall that $TM_{21}$ on average outperforms the other configurations, according to the results of Section IV. Also, at high AS, the BER curve slope remains the same for all the different configurations; therefore the level of diversity provided by the different configurations is the same. The diversity level also effects the trend of the BER curves for the proposed algorithm (proposed algorithm np-CSI) and the standard algorithm (standard algorithm np-CSI). Unlike the results from Fig.10(a), at high AS, the BER curve slope is the same for both systems; therefore, at high AS, the two systems are characterized by the same diversity order.

According to these results we can therefore conclude that the diversity order of a system that adopts the proposed algorithm falls in between the upper bound of a system that adopts a standard configuration selection algorithm and the lower bound of a system that employs non reconfigurable

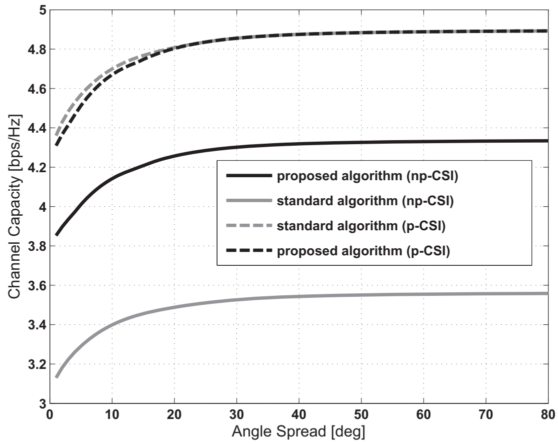


Fig. 9. Achievable channel capacity as a function of the angle spread (AS) for a 2 × 6 MIMO, with RCPAs (RCPA-1) at the receiver, that employs:(i) the proposed selection scheme including the effects of imperfect channel estimation (proposed algorithm np-CSI), (ii) the proposed selection scheme assuming perfect channel estimation (proposed algorithm p-CSI),(iii) an algorithm that selects the antenna configuration after estimating the channel for all possible configuration including the effects of imperfect channel estimation (standard np-CSI) and, (iv) a standard algorithm assuming perfect channel estimation (standard p-CSI). SNR = 5 dB.

antennas. On the other hand we observe that the proposed algorithm allows for better channel estimation (and thus, higher receiver SNR) than a standard configuration selection scheme.

## VII. Conclusion

A novel selection algorithm has been proposed in order to efficiently select the antenna configuration at the receiver of a MIMO system that employs reconfigurable antenna arrays. The proposed selection scheme allows the antenna configuration to be selected without the need of exhaustively estimating the channel transfer matrix for all possible array configurations and without the need to modify the pilot sequence of a conventional MIMO system making use of fixed antennas. The potential offered by this selection scheme has been demonstrated through simulations in a clustered channel model. A relative capacity gain is achievable with respect to a reconfigurable antenna MIMO system that selects the antenna configuration after estimating the channel for all the possible antenna configurations. In particular we have demonstrated that the higher the level of reconfigurability in the receiving antenna element, the higher the benefit offered by our proposed algorithm.

We have also shown that the functionality of this selection scheme is dependent on the differences existing between the antenna configurations of the reconfigurable antenna array. This fact motivates the need to develop reconfigurable antennas for MIMO systems jointly with the characteristics of the proposed selection algorithm.

Future work will involve validation of this configuration selection scheme through experimental results and will also consider the design of new reconfigurable antenna array architectures that fully exploit the proposed algorithm. Next steps will also concentrate on the application of the proposed configuration antenna selection procedure to multi element reconfigurable antenna system that exploit polarization and/or space diversity, instead of only pattern diversity. In this case, in fact, the ergodic channel capacity will depend on other wireless channel parameters rather than the only angle spread (e.g. channel polarization discrimination factor for polarization reconfigurable antennas).

## VIII. Acknowledgments

The authors would like to thank Alessandro Tomasoni and Prof. Sandro Bellini for their helpful discussions.

## References

[1] D. Piazza, N. Kirsch, A. Forenza, R. Heath Jr., and K. Dandekar, “Design and evaluation of a reconfigurable antenna array for MIMO systems," *IEEE Trans. Antennas Propag.*, vol. 56, no. 3, 2008.
[2] B. Cetiner, E. Akay, E. Sengul, and E. Ayanoglu, “A MIMO system with multifunctional reconfigurable antennas," *IEEE Antennas Wireless Propag. Lett.*, vol. 5, no. 31, pp. 463-466, 2006.
[3] B. Cetiner, H. Jafarkhani, J.-Y. Qian, H. J. Yoo, A. Grau, and F. De Flaviis, “Multifunctional reconfigurable MEMS integrated antennas for adaptive MIMO systems," *IEEE Commun. Mag.*, vol. 42, no. 12, pp. 62-70, 2004.
[4] A. Sayeed and V. Raghavan, “Maximizing MIMO capacity in sparse multipath with reconfigurable antenna arrays," *IEEE J. Select. Topics Signal Processing*, vol. 1, no. 1, pp. 156-166.
[5] D. Piazza, P. Mookiah, M. D'Amico, and K. Dandekar, “Two port reconfigurable circular patch antenna for MIMO systems," in *Proc. European Conf. Antennas Propagation, EUCAP*, 2007.
[6] A. Grau, H. Jafarkhami, and F. De Flaviis, “A reconfigurable multiple-input multiple-output communication system," *IEEE Trans. Wireless Commun.*, vol. 7, no. 5, 2008.
[7] A. Forenza and R. W. Heath Jr., “Benefit of pattern diversity via two-element array of circular patch antennas in indoor clustered MIMO channels," *IEEE Trans. Commun.*, vol. 54, no. 5, pp. 943-954, 2006.
[8] V. E. et al., “TGn channel models," *IEEE 802.11-03/940r4*, 2004.
[9] J. P. Kermoal, L. Schumacher, K. I. Pedersen, P. E. Mogensen, and F. Frederiksen, “A stochastic MIMO radio channel model with experimental validation," *IEEE J. Select. Areas Commun.*, vol. 20, no. 6, pp. 1211-1226, 2002.
[10] B. Hassibi and B. Hochwald, “How much training is needed in multiple-antenna wireless links?” *IEEE Trans. Inform. Theory*, vol. 49, no. 4, pp. 951-963, 2003.
[11] G. Golden, C. Foschini, R. Valenzuela, and P. Wolniansky, “Detection algorithm and initial laboratory results using V-BLAST space-time communication architecture," *Electron. Lett.*, vol. 35, no. 1, pp. 14-16, 1999.
[12] D. Samardzija, C. Papadias, and R. Valenzuela, “Experimental evaluation of unsupervised channel deconvolution for wireless multiple-transmitter/multiple-receiver systems," *Electron. Lett.*, vol. 38, no. 20, pp. 1214-1216, 2002.
[13] A. Adjoudani, E. Beck, A. Burg, G. Djuknic, T. Gvoth, D. Haessig, S. Manji, M. Milbrodt, M. Rupp, D. Samardzija, A. Siegel, I. Sizer, T., C. Tran, S. Walker, S. Wilkus, and P. Wolniansky, “Prototype experience for MIMO BLAST over third-generation wireless system," *IEEE J. Select. Areas Commun.*, vol. 21, no. 3, pp. 440-51, 2003.
[14] D. Samardzija and N. Mandayam, “Pilot-assisted estimation of MIMO fading channel response and achievable data rates," *IEEE Trans. Signal Processing*, vol. 51, no. 11, pp. 2882-2890, 2003.
[15] L. Musavian, M. Nakhai, M. Dohler, and A. Aghvami, “Effect of channel uncertainty on the mutual information of MIMO fading channels," *IEEE Trans. Veh. Technol.*, vol. 56, no. 5, Sept. 2007.
[16] R. Vaughan, “Two-port higher mode circular microstrip antennas," *IEEE Trans. Antennas Propag.*, vol. 36, no. 3, pp. 309-21, 1988.
[17] R. Vaughan and J. Andersen, “Antenna diversity in mobile communications," *IEEE Trans. Veh. Technol.*, vol. T-36, no. 4, pp. 149-172, 1987.
[18] C. Waldschmidt, J. Hagen, and W. Wiesbeck, “Influence and modelling of mutual coupling in MIMO and diversity systems," *IEEE Antennas Propagation Society, AP-S International Symposium (Digest)*, vol. 3, pp. 190-193, 2002.
[19] I. Bahl and P. Bhartia, *Microstrip Antennas*. Artech House, 1980.
[20] L. M. Correia, *Wireless Flexible Personalized Communications*. John Wiley and Sons, Inc., 2001.

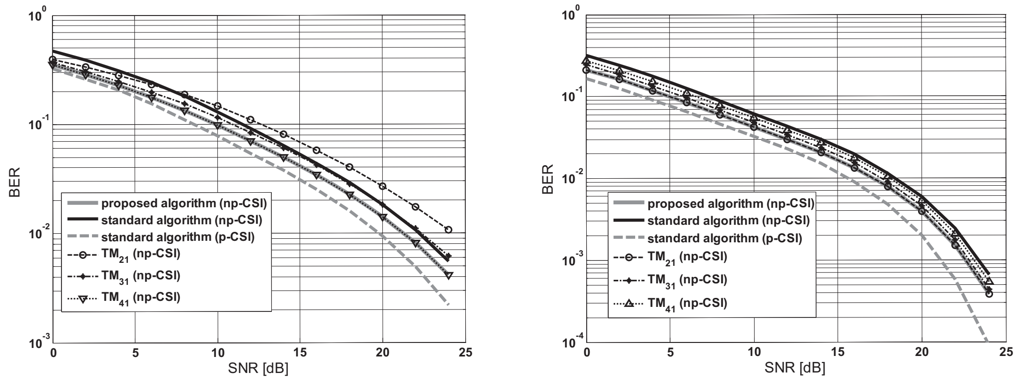


Fig. 10. BER versus SNR for a $2 \times 2$ MIMO system, with RCPA-1 at the receiver, that employs:(i) the proposed selection scheme including the effects of imperfect channel estimation (proposed algorithm np-CSI), (ii) an algorithm that selects the antenna configuration after estimating the channel for all possible configuration including the effects of imperfect channel estimation (standard np-CSI) and, (iii) a standard algorithm assuming perfect channel estimation (standard p-CSI). The BER curves relative to non reconfigurable circular patch antennas operating in different modes assuming non-perfect channel estimation are also reported. (a) AS=$10^o$ and (b) AS=$60^o$.

[21] M. Bengtsson, D. Astely, and B. Ottersten, “Measurements of spatial characteristics and polarization with a dual polarized antenna array," in *Proc. IEEE Veh. Technol. Conf.*, vol. 1, pp. 366-370, 1999.

[22] A. Forenza, A. Pandharipande, H. Kim, and R. Heath Jr., “Adaptive MIMO transmission scheme: exploiting the spatial selectivity of wireless channels," in *Proc. IEEE 61st Veh. Technol. Conf.*, vol. 5, pp. 3188-92, 2005.

[23] K. Yu, M. Bengtsson, B. Ottersten, D. McNamara, P. Karlsson, and M. Beach, “Modeling of wide-band MIMO radio channels based on NLoS indoor measurements," *IEEE Trans. Veh. Technol.*, vol. 53, no. 3, pp. 655-65, 2004.

[24] M. Ivrlac, T. Kurpjuhn, C. Brunner, and W. Utschick, “Efficient use of fading correlations in MIMO systems," in *Proc. IEEE 54th Veh. Technol. Conf.*, vol. 4, pp. 2763-7, 2001.

[25] M. Herdin and E. Bonek, “A MIMO correlation matrix based metric for characterizing non-stationarity," *IST Mobile Wireless Commun. Summit*, 2004.

**Daniele Piazza** (S'03) received the B.S. degree in telecommunication engineering from Politecnico di Milano, Italy, in 2003. In 2006 he received the Laurea degree with high honors in telecommunication engineering, with specialization in radio frequency communications, from Politecnico di Milano, Italy, and the M.S. degree in electrical and computer engineering from Drexel University in Philadelphia, Pennsylvania, where he conducted research focused on reconfigurable antennas for MIMO communications.

He is currently with Drexel University, where he is pursuing his PhD degree in electrical and computer engineering developing reconfigurable antenna systems for adaptive MIMO communications. He is also working as a researcher at Politecnico di Milano in the field of antennas. His research interests concentrate mainly on MIMO antenna design, reconfigurable antennas, smart antenna arrays and MIMO communications.

**John Kountouriotis** received the B.Sc degree from the National Technical University of Athens in 2004 and the M.Sc from Drexel University in 2006, both in Electrical and Computer Engineering. He is currently with Drexel University Wireless Systems Laboratory working towards his Ph.D degree. His research interests include MIMO communication systems, ad hoc networks and adaptive signaling.

**Michele D'Amico** was born in Italy in 1965. He received the M.S. degree in Electronic Engineering from the Politecnico di Milano in 1990, and the Ph.D. degree in Mathematics from the University of Essex (UK) in 1997. He was Assistant Professor at Dipartimento di Elettronica e Informazione (DEI) of Politecnico di Milano from 1993 to 2002. He has been visiting researcher at the European Space Agency (ESA/ESTEC) and at the Rutherford Appleton Laboratory (UK). Since 2002 he has been Associate Professor of Applied Electromagnetics at DEI. His research interests include radarmeteorology, electromagnetic wave propagation in the troposphere and antennas. Since May 2004 he has been responsible for the experimental activities of the CE.S.A.R.E. laboratory of the Politecnico di Milano, located in Busto Arsizio, and dedicated mainly to Electromagnetic Compatibility (EMC).

**Kapil R. Dandekar** (S'95, M'01, SM'07) received the B.S. degree in electrical engineering from the University of Virginia in 1997 with specializations in communications and signal processing, applied electrophysics, and computer engineering. He received the M.S. and Ph.D. degrees in Electrical and Computer Engineering from the University of Texas at Austin in 1998 and 2001, respectively. In 1992, he worked at the U.S. Naval Observatory and from 1993-1997, he worked at the U.S. Naval Research Laboratory.

In 2001, Dandekar joined the Electrical and Computer Engineering Department at Drexel University in Philadelphia, Pennsylvania. He is currently an Associate Professor and the Director of the Drexel Wireless Systems Laboratory (DWSL). DWSL has been supported by the U.S. National Science Foundation, Army CERDEC, National Security Agency, Office of Naval Research, and private industry. Dandekar's current research interests involve MIMO ad hoc networks, reconfigurable antennas, free space optical communications, ultrasonic communications, and sensor networks. He has published articles in several journals including IEEE TRANSACTIONS ON ANTENNAS AND PROPAGATION, IEEE TRANSACTIONS ON WIRELESS COMMUNICATIONS, IEEE TRANSACTIONS ON COMMUNICATIONS, IEEE TRANSACTIONS ON VEHICULAR TECHNOLOGY, and IEE ELECTRONICS LETTERS. Dandekar currently serves on the editorial board of IEEE Expert Now and also serves on the IEEE Educational Activities Board.